Research Article | Vol. 9, No. 6 | 1 Jun 2018 | BIOMEDICAL OPTICS EXPRESS 2733
Biomedical Optics EXPRESS

Diagnosis of dermatophytosis using single fungus endogenous fluorescence spectrometry

FEI YE,[1] MEIRONG LI,[2] SIQI ZHU,[1] QINGLIANG ZHAO,[3,4] AND JINGANG ZHONG[1,5]

[1]*Department of Optoelectronic Engineering, Jinan University, Guangzhou 510632, China*
[2]*Department of Dermatology, Third Affiliated Hospital, Sun Yat-sen University, Guangzhou 510630, China*
[3]*State Key Laboratory of Molecular Vaccinology and Molecular Diagnostics & Center for Molecular Imaging and Translational Medicine, School of Public Health, Xiamen University, Xiamen 361102, China*
[4]*zhaoql@xmu.edu.cn*
[5]*tzjg@jnu.edu.cn*

Abstract: We propose to use a single fungus endogenous fluorescence spectrometry base on a hyperspectral fluorescence microscope for the diagnosis of dermatophytosis. Dermatophyte samples, including *Aspergillus, Trichophyton rubrum, Microsporum gypseum, and Microsporum canis* were imaged, and the endogenous fluorescence spectrum of a single fungus was calculated. High contrast fluorescence images and endogenous fluorescence spectrum of the single fungus were used to identify the type of dermatophyte. Morphologically similar *Microsporum gypseum* and *Microsporum canis* can be distinguished using an endogenous fluorescence spectrum of the single fungus. Meanwhile, our result showed that the sensitivity and specificity of identifying *Microsporum gypseum* were 95% and 93%, and the sensitivity and specificity of identifying *Microsporum canis* were 94% and 93%.

OCIS codes: (170.0170) Medical optics and biotechnology; (110.4234) Multispectral and hyperspectral imaging; (180.2520) Fluorescence microscopy; (170.6935) Tissue characterization.

References and links

1. B. Havlickova, V. A. Czaika, and M. Friedrich, "Epidemiological trends in skin mycoses worldwide," Mycoses **51**(Suppl 4), 2–15 (2008).
2. J. R. Estela Cubells, A. M. Victoria Martínez, L. Martínez Leboráns, and V. Alegre de Miquel, "Fluorescence Microscopy as a Diagnostic Tool for Dermatophytosis," Am. J. Dermatopathol. **38**(3), 208–210 (2016).
3. F. Lanternier, S. Pathan, Q. B. Vincent, L. Liu, S. Cypowyj, C. Prando, M. Migaud, L. Taibi, A. Ammar-Khodja, O. B. Stambouli, B. Guellil, F. Jacobs, J. C. Goffard, K. Schepers, V. Del Marmol, L. Boussofara, M. Denguezli, M. Larif, H. Bachelez, L. Michel, G. Lefranc, R. Hay, G. Jouvion, F. Chretien, S. Fraitag, M. E. Bougnoux, M. Boudia, L. Abel, O. Lortholary, J. L. Casanova, C. Picard, B. Grimbacher, and A. Puel, "Deep Dermatophytosis and Inherited CARD9 Deficiency," N. Engl. J. Med. **369**(18), 1704–1714 (2013).
4. M. H. Idriss, A. Khalil, and D. Elston, "The diagnostic value of fungal fluorescence in onychomycosis," J. Cutan. Pathol. **40**(4), 385–390 (2013).
5. H. Cardillo, J. Kohler, E. Kriner, and K. Mehta, "Applications of Wood's Lamp technology to detect skin infections in resource-constrained settings," in Global Humanitarian Technology Conference, (2014), 548–554.
6. G. Kaufman, B. A. Horwitz, R. Hadar, Y. Ullmann, and I. Berdicevsky, "Green fluorescent protein (GFP) as a vital marker for pathogenic development of the dermatophyte Trichophyton mentagrophytes," Microbiology **150**(Pt 8), 2785–2790 (2004).
7. M. A. Lopes, O. Fischman, W. Gambale, and B. Corrêa, "Fluorescent method for studying the morphogenesis and viability of dermatophyte cells," Mycopathologia **156**(2), 61–66 (2002).
8. J. L. Mann, "Autofluorescence of Fungi: An Aid to Detection in Tissue Sections," Am. J. Clin. Pathol. **79**(5), 587–590 (1983).
9. M. S. Ammor, "Recent Advances in the Use of Intrinsic Fluorescence for Bacterial Identification and Characterization," J. Fluoresc. **17**(5), 455–459 (2007).

#320718 https://doi.org/10.1364/BOE.9.002733
Journal © 2018 Received 26 Jan 2018; revised 13 Apr 2018; accepted 27 Apr 2018; published 21 May 2018

Biomedical Optics EXPRESS

10. Y. R. Zhao, K. Q. Yu, X. Li, and Y. He, "Detection of Fungus Infection on Petals of Rapeseed (Brassica napus L.) Using NIR Hyperspectral Imaging," Sci. Rep. **6**(1), 38878 (2016).
11. D. Bannon, "Hyperspectral imaging: Cubes and slices," Nat. Photonics **3**(11), 627–629 (2009).
12. S. Zhu, K. Su, Y. Liu, H. Yin, Z. Li, F. Huang, Z. Chen, W. Chen, G. Zhang, and Y. Chen, "Identification of cancerous gastric cells based on common features extracted from hyperspectral microscopic images," Biomed. Opt. Express **6**(4), 1135–1145 (2015).
13. S. Zhu, K. Su, M. Li, Z. Chen, H. Yin, and Z. Li, "Multi-type hyper-spectral microscopic imaging system," Optik - International Journal for Light and Electron Optics **127**(18), 7218–7224 (2016).
14. Q. Li, Z. Sun, Y. Wang, H. Liu, F. Guo, and J. Zhu, "Histological skin morphology enhancement base on molecular hyperspectral imaging technology," Skin research and technology: official journal of International Society for Bioengineering and the Skin (ISBS) [and] International Society for Digital Imaging of Skin (ISDIS) [and] International Society for Skin Imaging **20**(I), 332–340 (2013) (and).
15. H. Tu, Y. Liu, D. Turchinovich, M. Marjanovic, J. Lyngsø, J. Lægsgaard, E. J. Chaney, Y. Zhao, S. You, W. L. Wilson, B. Xu, M. Dantus, and S. A. Boppart, "Stain-free histopathology by programmable supercontinuum pulses," Nat. Photonics **10**(8), 534–540 (2016).
16. H. Leung and S. Haykin, "The complex backpropagation algorithm," Signal Processing IEEE Transactions on **39**(9), 2101–2104 (1991).

1. Introduction

Dermatophytosis is a superficial fungal infection of the keratinized tissues. The World Health Organization estimates that approximately 25 percent of the population worldwide suffers from different kinds of fungal infections [1]. The major sites of infection include the epidermis, hair, and nails. Dermatophytosis is usually caused by dermatophytes, including *Aspergillus, Trichophyton rubrum, Microsporum gypseum, and Microsporum canis.* Superficial fungal infections are not necessarily life-threatening. However, they can cause itching, inflammation, and redness, which may significantly reduce the quality of life. If the diagnosis and treatment of dermatophytosis is not appropriate, the dermatophytes can possibly spread to deeper tissues, resulting in systemic infections [1–3].

Several methods of detecting dermatophytes are currently available [2–4]. One of the methods in clinical use is direct microscopic examination of clinical specimens removed from a lesion, which is a rapid diagnostic method. However, as a result of its low contrast, it is easy for inexperienced diagnosticians to miss positive diagnoses. In vitro cultures combined with microscopic examinations are specific diagnostic methods, but they are very time-consuming, and it may take up to 8 weeks to obtain the results. Another diagnostic approach involves using fluorescence microscopy. In this method, the tissues are stained with periodic acid Schiff (PAS) for visualization of the fungal structures, however, this method is expensive and requires special reagents. Long-wave ultraviolet (UV) light sources can stimulate the fluorescence of dermatophytosis, and this method is currently used as a screening procedure [5–8]. The Wood's Lamp is a common first-step modality used for diagnosing skin infections. This method constitutes a clinical application of long-wave UV light that is emitted in the 365-400 nm range and is commonly used by dermatologists to diagnose various pigmented and infectious disorders. The diagnostic criteria for the Wood's lamp are mainly dependent on the skin color visualized under fluorescent light. However, the color of infected skin can be hard to judge under UV light for many fungal infections, which may lead to ambiguous conclusions. Therefore, it would be important to develop a rapid, accurate, and low-cost method for the diagnosis of dermatophytosis.

Dermatophytes have numerous endogenous molecules at specific excitation and emission wavelengths that make them very suitable probes for biological detection and characterization. These endogenous fluorophores include tryptophan in proteins, other amino acids (tyrosine and phenylalanine), nucleic acids, and co-enzymes [9].

Hyperspectral fluorescence microscopy (HFM) employs a long-wave UV light source to illuminate the biological materials. Some intrinsic fluorescent substances can be absorbed by the photon energy of exciting light and emit longer wavelength visible photons. The objective lens collects a set of narrow spectral band images. These images are combined to form a three-dimensional (x, y, λ) hyperspectral data cube, where x and y represent two spatial

Biomedical Optics EXPRESS

dimensions, and λ represents the spectrum dimension (comprising a range of wavelengths) [10–13]. Compared to the traditional wide spectral band imaging technology, hyperspectral imaging collects all the images of the narrow spectral band over a continuous spectrum range and produces the spectra of all pixels in the scene. The fluorescence spectrum reflects the chemical composition of the sample. It has the advantage of producing a spectrum for each pixel in the image, which can be used to classify the materials that cannot be identified using traditional methods [14]. Therefore, hyperspectral imaging technology can be used in dermatology with the goal of enhancing objective assessments and diagnostic accuracy.

In this study, we proposed a single fungus endogenous fluorescence spectrometry (SFEFS) for the diagnosis of dermatophytosis. A hyperspectral fluorescence imaging system based on the acousto-optic tunable filter (AOTF) was used to capture a set of narrow band fluorescence images of a dermatophytosis specimen. Dermatophytes, including *Aspergillus, Trichophyton rubrum, Microsporum gypseum*, and *Microsporum canis* were imaged with their endogenous fluorescence. Meanwhile, the spectrum of a single fungus was acquired. This method has high sensitivity and specificity for the diagnosis of dermatophytosis. Unlike traditional RGB color imaging methods [14], the proposed method combines high contrast fluorescence images and the quantitative spectrum of a single fungus. As a new method, it can be used to help the dermatologist perform morphological and histological analyses. Since the sample did not require dyeing, it simplified the steps of operation, while reducing time and cost [15]. Compared to the Wood's lamp, HFM can offer microscopic images of a single fungus with quantitative spectral information and supply reliable diagnostic information for the dermatologist. To the best of our knowledge, this is the first report of single fungus endogenous fluorescence spectrometry used in the diagnosis of dermatophytosis.

2. Materials and methods

2.1 Materials

We included 10 cases of dermatophytosis diagnosed in the Department of Dermatology at the Third Affiliated Hospital of Sun Yat-sen University, Guangzhou, China. The available information included the clinical diagnosis based on the biopsy results, the patient's age and sex, and the location of the infection. All volunteers were informed of the aims and risks of the study and provided their written consent. Ethics approval was granted by the Third Affiliated Hospital, Sun Yat-sen University, Guangzhou, China.

When obtaining specimens from the patients, we first treated the lesions using a 75% ethanol disinfection process, and then used a blade to scrape the edges of skin lesions. The specimens were placed on glass slides with 1 drop of a 10% potassium hydroxide solution. A micro-heating, light pressure glass cover slide was placed on top of the specimen. Thirty minutes after the slide preparation, the samples were put under the HFM to be imaged. Meanwhile, all the samples were cultured and confirmed using molecular verification. DNA was extracted using the UltraClean microbial DNA isolation kit (MoBio, Carlsbad, CA, U.S.A.) according to the manufacturer's instructions. After the DNA concentration was measured, a PCR reaction system was set up using a kit (THUN-DERBIRD SYBR qPCR MixKit). ITS (internal transcribed spacer) rDNA was amplified using primers ITS4 (5′-TCCTCCGCTTATTGATATGC-3′) and ITS5 (5′-GGAAGTAAA-AGTCGTAACAAGG-3′) for *Aspergillus*. ITS rDNA was amplified using primers ITS1 (5′-TCCGTAGGTGAACCTGCGC-3) and ITS4 (5′-TCCTCCGCTTATTGATATGC-3′) for *Trichophyton rubrum, Microsporum gypseum, and Microsporum canis.* The sequences were compared to GenBank and through a local blast with a molecular database maintained for research purposes at the CBS-KNAW Fungal Biodiversity Centre, Utrecht, Netherlands. The resulting strains were subjected to ITS identification. Among the 10 phenotype-identified strains, the ITS sequence was compared with the database, and the sequence similarity was greater than 98.0%.

Biomedical Optics EXPRESS

To make a composite sample of *Microsporum gypseum* and *Microsporum canis*, we took a *Microsporum gypseum* sample on the specimen slide, and then added a *Microsporum canis* sample. A drop of 10% potassium hydroxide solution was added in the sample. A micro-heating, light pressure glass cover slide was placed on top of the specimen. Thirty minutes later, we put the samples under the HFM to be observed.

2.2 Instrument setup

The structure of the experimental setup is shown in Fig. 1(A). The hardware of the system comprises the following: a 2/3-inch complementary metal oxide semiconductor (CMOS) camera (HAMAMATSU C11440-42U) with an image size of 2048 × 2048 pixels (pixel size of 6.5 μm × 6.5 μm); a liquid crystal tunable filter (LCTF) (CRI.INC, VariSpec VIS) that covered the of 420–720 nm spectrum range with spectral resolution of 8 nm; a dichroic mirror (Thorlabs, Inc., DMLP425R) to separate the UV light and the optical signal; a 40x infinity-corrected imaging microscope objective with an N.A. of 0.65 (Olympus, Inc.); two different light sources for spectroscopy; A 130W xenon lamp combined with a narrowband-pass filter centered at 263 nm was used to obtain the fluorescence spectral images; a white 5W LED light source with the power of was used for transmission spectroscopy. Our own custom-developed software was used to control the gain factor, exposure time, sweep range, and step length. The minimum step length of the spectrum scanning and the maximum acquisition speed of the system were 2 nm and 50 ms, respectively, as determined by the LCTF characteristics. The exposure time of the system was adjustable from 1/44000 - 115 s.

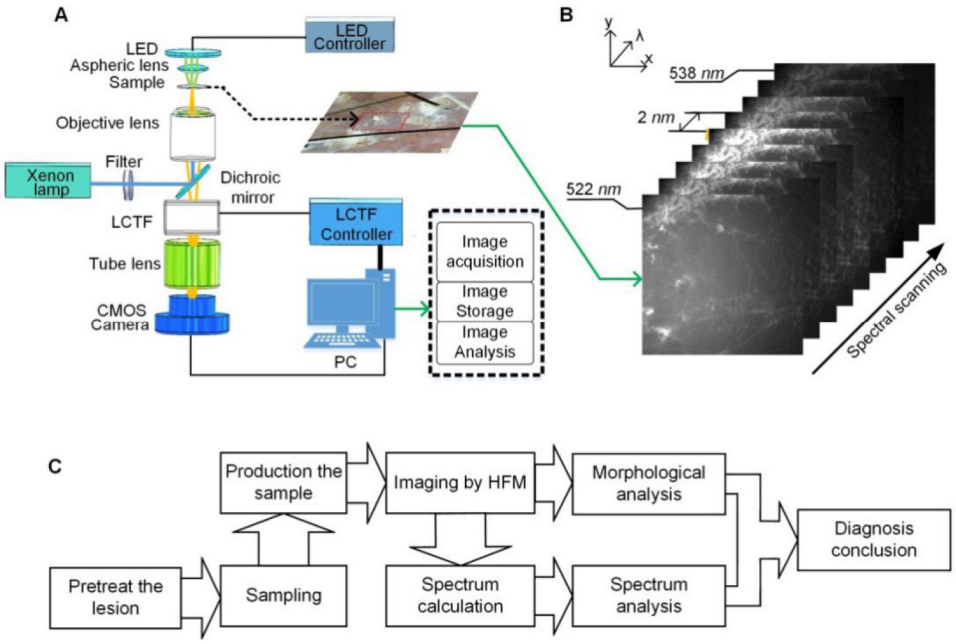

Fig. 1. Schematic diagram of hyperspectral fluorescence microscopy. A. The experimental setup of hyperspectral microscope. B. Three-dimensional hyperspectral data cube. C. The process of diagnosis of dermatophytosis. LCTF: liquid crystal tunable filter; CMOS: complementary metal oxide semiconductor; LED: light-emitting diode; PC: personal computer

2.3 Data acquisition

To capture the hyperspectral fluorescence images, the skin tissue specimen was placed on the stage of the HFM and then illuminated with UV light. The stimulated fluorescence light from the specimen was initially collected via the objective lens of the microscope, filtered with the AOTF adapter, and then imaged using the CMOS detector. With the wavelength switching at

Biomedical Optics EXPRESS

narrow bandwidths from 420 to 720 nm by the AOTF adapter, different single-band images could be captured by the CMOS detector. In this study, 150 single-band images of each scene of the skin sections were captured and stored in sequential band format. One scene of the hyperspectral images could be visualized as a 512 × 512 × 150 (12-bit) three-dimensional data cube, which is shown in Fig. 1(B). The scenes contained both spectral and spatial information to potentially obtain high-contrast images of dermatophytes for histological analysis.

2.4 Hyperspectral data analysis

The image processing software on the computer was written in MATLAB (MathWorks, 2012), which includes image preprocessing, analyzing, and displaying features. After image acquisition, preprocessing was performed to remove some of the effects. Next, the raw hyperspectral images acquired by CMOS detectors were corrected using baseline subtraction. The raw hyperspectral images were subtracted from a dark field image. According to the spectral response of the CMOS detector, we corrected the hyperspectral images. The corrected hyperspectral images were used for spectrum calculation. We chose a point in a fluorescence image for spectrum calculation. The pixel in the image comprised a continuous spectrum that could be extracted by the MATLAB computer program to provide the spectrum data. We identified the signal intensity value of all the wavelengths at the chosen point and found the maximum signal intensity. We then used the corresponding wavelengths for fluorescence intensity normalization. In this research, the normalized fluorescence spectrum was used in spectral analysis.

To help the dermatologist analyze the hyperspectral data, our own custom-developed software had basic data processing functions including data cube import, single band image display, spectrum extract, and result exporting.

In this study, we used the sum of the Euclidean distance between two spectra to describe the spectrum differences between the samples [13]. The calculation for this distance is expressed below:

$$D=\sum_{k=1}^{n}\sqrt{(F_{1k}-F_{2k})^2}$$

Here, F_{1k} and F_{2k} denote the fluorescence intensity of any two given samples at a certain wavelength, and n denotes the total number of wavelengths.

In this study, we used a custom-made program based on the backpropagation algorithm to identify the type of dermatophyte [12, 16].

The process of diagnosing dermatophytosis from our methods here included preparing and imaging the sample, analyzing the spectrum, and arriving at a diagnostic result, as is shown in Fig. 1(C).

3. Results

3.1 Comparison of bright-field imaging and fluorescence imaging

An *Aspergillus* specimen taken from a patient with dermatophytosis was first illuminated using the white LED light, and then imaged using the bright-field microscopy system. Next the specimen was illuminated with UV light and a set of narrow spectral band fluorescence images were acquired. Using our own custom-developed data processing program, the spectrum of a single point was acquired. Figure 2(A) shows the bright-field image of *Aspergillus*. Figure 2(B) shows the fluorescence image of *Aspergillus* at 560 nm. Compared to the bright-filed image shown in Fig. 2(A), the fluorescence image in Fig. 2(B) has better contrast. The signal-to-noise ratio (SNR) of points A, B, and C from Figs. 2(A) and 2(B) were calculated and are shown in Fig. 2(C). The spectral band of the fluorescence imaging was 2 nm. From the three-dimensional hyperspectral data cube, we calculated the spectrum for each

Biomedical Optics EXPRESS

single point in the image. Points A, B, and C of *Aspergillus* shown in Fig. 2(A) were selected to calculate the spectrum. Figure 2(D) shows the fluorescence spectra of points A, B, and C. The fluorescence spectrum of *Aspergillus* could be used to identify the type of fungus.

We used the average method for calculating the spectrum for a point, and the average spectra of a point was calculated using the spectra of the 25 nearby pixel points. We tried to find the strongest fluorescence signal center position of the sample to measure the spectrum. Points A, B, and C are the center positions of the strongest fluorescence signal. Points A and C are the locations of fungal conidiophore, and point B is the location of the fungal hyphae. Conidiophore and hyphae are the different parts of the fungus. Hyphae absorb nutrients, including various proteins. The conidiophore is the main fungal reproductive organ and requires large amounts of nutrients. Little difference is found in the fluorescence spectra of points A, B, and C. The fluorescence is possibly emitted by various nutrients, including various amino acids.

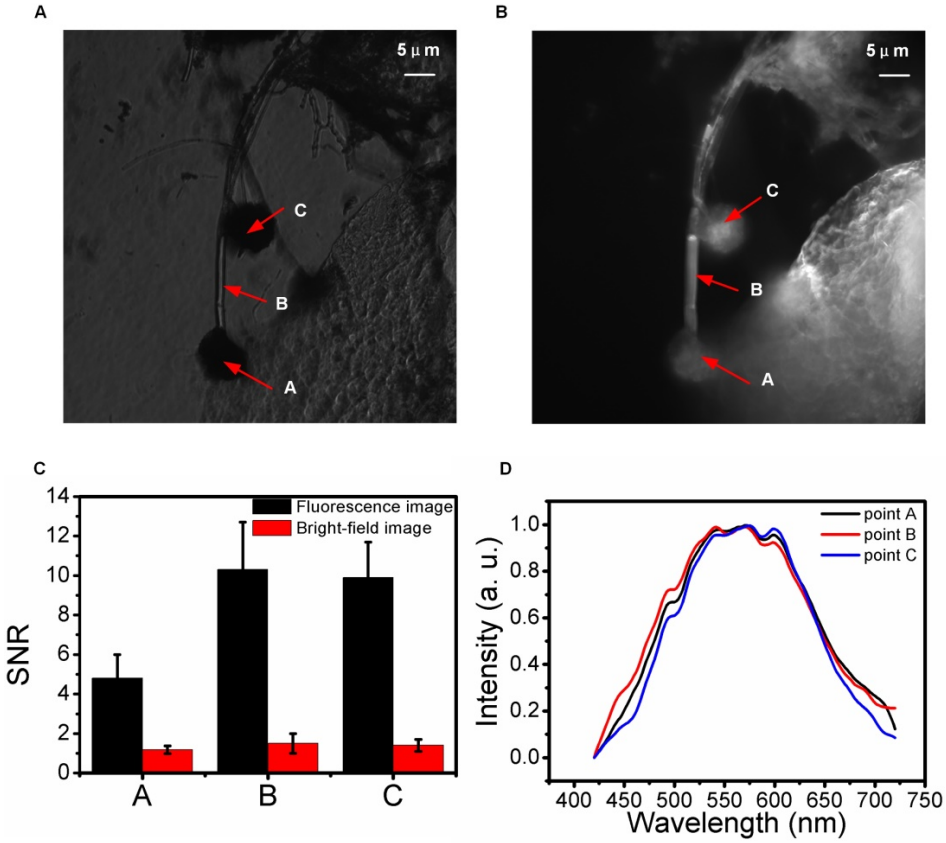

Fig. 2. Bright-field and hyperspectral fluorescence imaging of Aspergillus. A. Bright-field image of Aspergillus. B. Fluorescence image of Aspergillus of 560 nm. C. SNR of points A, B, C. D. The fluorescence spectra of points A, B, and C. SNR: signal-to-noise ratio.

3.2 Hyperspectral fluorescence imaging of dermatophytes

A. Hyperspectral fluorescence imaging of *Trichophyton rubrum*

A *Trichophyton rubrum* specimen obtained from a patient with dermatophytosis was first imaged using the bright-field microscopy system. The specimen was illuminated with UV light and a series of narrow band fluorescence images were acquired. Figure 3(A) shows the bright-field image of *Trichophyton rubrum*. Figure 3(B) shows the fluorescence image of

Biomedical Optics EXPRESS

Trichophyton rubrum of 630 nm. Figure 3(D) shows a series of narrow band fluorescence images of the specimen. From the three-dimensional hyperspectral data cube, we calculated the spectrum for each point in the image. Points A, B, and C of *Trichophyton rubrum* shown in Fig. 3(A) were selected to calculate the spectrum. Figure 3(C) shows the fluorescence spectra of points A, B, and C. The fluorescence spectrum of *Trichophyton rubrum* could be used for identifying the type of fungus.

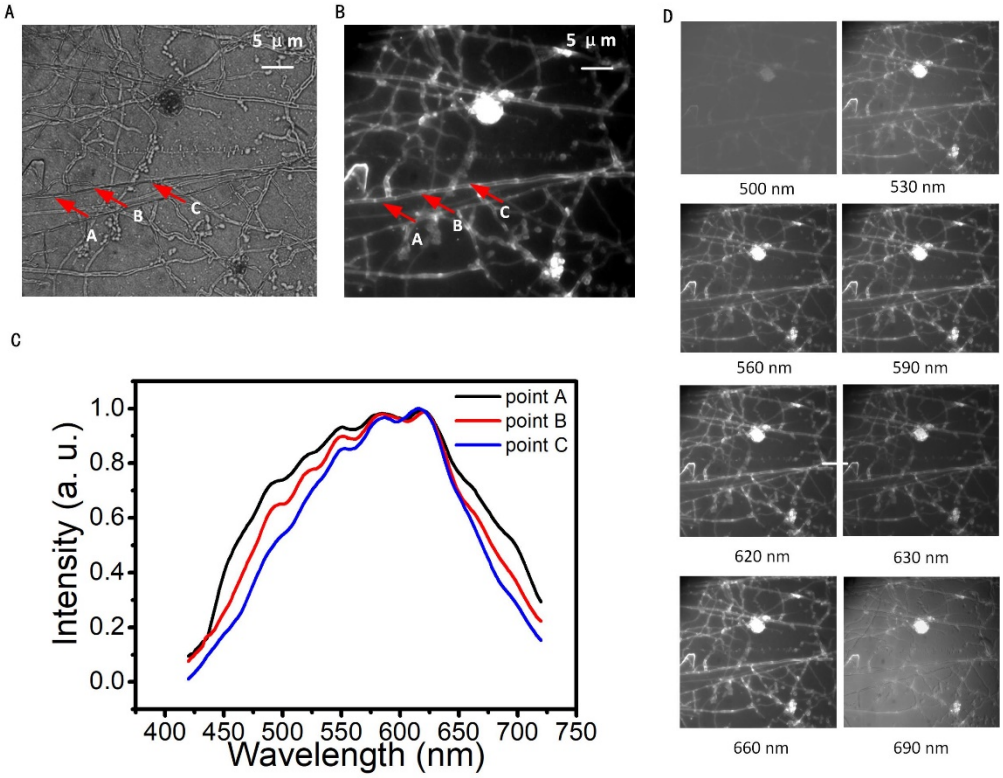

Fig. 3. Bright-field and hyperspectral fluorescence imaging of *Trichophyton rubrum*. A. Bright-field image of *Trichophyton rubrum*. B. Fluorescence image of *Trichophyton rubrum* of 560 nm. C. The fluorescence spectra of points A, B, and C. D. A series of narrow spectral band fluorescence images of *Trichophyton rubrum*.

B. Hyperspectral fluorescence imaging of Microsporum gypseum and Microsporum canis

Three *Microsporum gypseum* specimens obtained from patients with dermatophytosis were first imaged using the bright-field microscopy system. The specimens were illuminated with UV light and a set of narrow band images were acquired. Figure 4(A) shows one bright-field image of the *Microsporum gypseum* specimens. Figure 4(B) shows one fluorescence image of *Microsporum gypseum* at 580 nm. Figure 4(C) shows the average fluorescence spectra of the *Microsporum gypseum* specimens. Three *Microsporum canis* specimens obtained from patients with dermatophytosis were first imaged using the bright-field microscopy system. The specimens were illuminated with UV light and a set of narrow band fluorescence images were acquired. Figure 4(D) shows one bright-field image of the *Microsporum canis* specimens. Figure 4(E) shows one fluorescence image of the *Microsporum canis* specimens at 530 nm. Figure 4(F) shows the average fluorescence spectra of the *Microsporum canis* specimens. In this study, the spectrum of *Microsporum gypseum* in Fig. 4(C) and the spectrum of *Microsporum canis* in Fig. 4(F) are used as standard spectra for comparison. S_{mg}

Biomedical Optics EXPRESS

is the standard spectra of *Microsporum gypseum* and S_{mc} is the standard spectra of *Microsporum canis*. Morphologically, *Microsporum gypseum,* and *Microsporum canis* are very similar, and it may be difficult for an inexperienced doctor to distinguish them from each other. However, the spectra of *Microsporum gypseum* and *Microsporum canis* are different, as shown in Figs. 4(C) and 4(F). With the spectra data, we could clearly distinguish each one from the other.

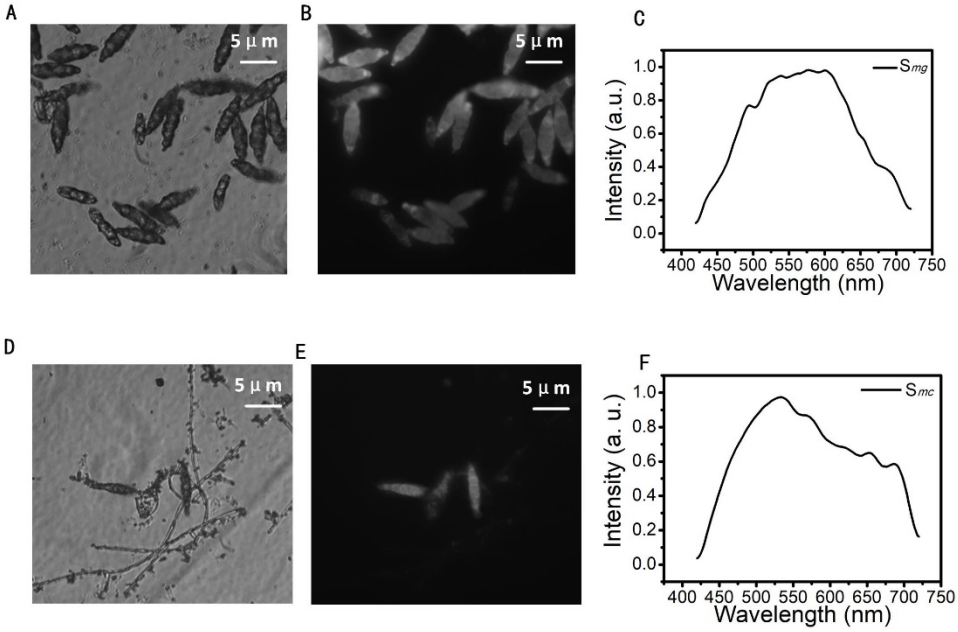

Fig. 4. Bright-field and hyperspectral fluorescence imaging of *Microsporum gypseum* and *Microsporum canis*. A. Bright-field image of *Microsporum gypseum*. B. Fluorescence image of *Microsporum gypseum* at 580 nm. C. The average fluorescence spectra of *Microsporum gypseum*. S_{mg} is the standard spectra of *Microsporum gypseum*. D. Bright-field image of *Microsporum canis*. E. Fluorescence image of *Microsporum canis* at 530 nm. F. The average fluorescence spectra of *Microsporum canis*. S_{mc} is the standard spectra of *Microsporum canis*.

3.3 Identifying the type of dermatophytes by HFM

To demonstrate the identification of the different types of dermatophytes using HFM, a composite sample containing *Microsporum gypseum* and *Microsporum canis* was made and imaged using HFM. Figure 5(A) shows the bright-field image of the composite specimen. Figure 5(B) shows the fluorescence image of composite specimen at 570 nm. Figure 5(C) shows the fluorescence spectra of points A1, A2, A3, B1, B2, and B3 of the specimen. Figure 5(D) shows a series of narrow spectral band fluorescence images of the composite sample. From the bright-field image shown in Fig. 5(A), it is difficult to distinguish the two types of fungus. However, from the spectra graph in Fig. 5(C), we found that the spectra of points A1, A2, and A3 are different from the spectra of points B1, B2, and B3. Points A1, A2, and A3 belong to a specific fungus, and points B1, B2, and B3 belong to another specific fungus.

We compared the spectra of the 6 points and calculated the Euclidean distance of the fluorescence spectra between the two types of dermatophytes. Table 1 shows the Euclidean distance of the different spectra. D_{mg} is the spectral Euclidean distance between the sample and S_{mg}. D_{mc} is the spectral Euclidean distance between the sample and S_{mc}. From Table 1, we concluded that the spectral Euclidean distance is significantly greater between two types of dermatophytes. Therefore, we concluded that the samples of A1, A2, and A3 contained *Microsporum canis*, and the samples of B1, B2, and B3 contain *Microsporum gypseum*.

Biomedical Optics EXPRESS

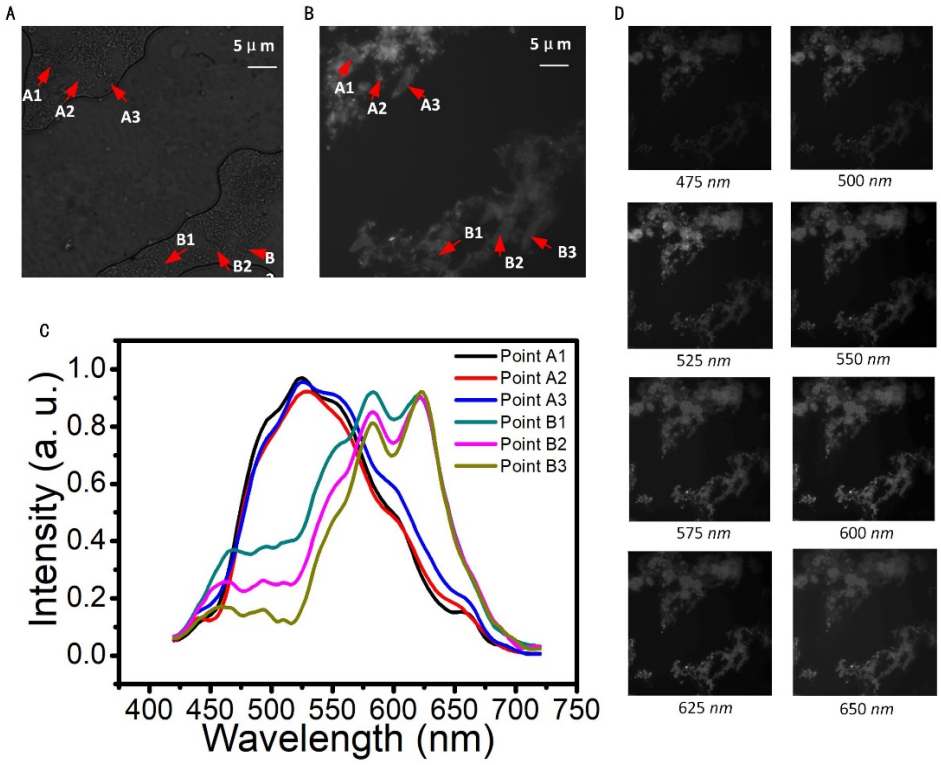

Fig. 5. Bright-field and hyperspectral fluorescence imaging of the composite sample containing *Microsporum gypseum* and *Microsporum canis*. A. Bright-field image. B. Fluorescence image. C. The fluorescence spectra of points A1, A2, A3, B1, B2, and B3. D. A series of narrow spectral band fluorescence images of the composite sample.

Table 1. The Euclidean distance of different spectra

	A1	A2	A3	B1	B2	B3
D_{mg}	33.36	30.35	32.71	8.18	6.25	7.89
D_{mc}	12.05	11.23	13.3.	29.58	28.25	29.55

Table 2. Accuracy of identification *Microsporum gypseum* and *Microsporum canis* by different standard spectra.

Target dermatophyte	Sensitivity	Specificity
Microsporum gypseum	95%	93%
Microsporum canis	94%	93%

In this case, we used a custom-made program based on the backpropagation algorithm to identify the type of dermatophyte. We used a hundred groups of data, twenty groups of training data of *Microsporum gypseum* and another twenty groups of training data of *Microsporum canis*. The sensitivity and specificity of the identification methods are shown in Table 2. When identifying *Microsporum gypseum*, the sensitivity and specificity were 95% and 93%. When identifying *Microsporum canis*, the sensitivity and specificity were 94% and 93%.

Biomedical Optics EXPRESS

4. Discussion and conclusion

The fungus and its metabolites contain endogenous fluorescent substances, which are used as markers of hyperspectral fluorescence imaging. These endogenous fluorophores include tryptophan, tyrosine, phenylalanine, nucleic acids, and coenzymes. These substances have unique fluorescence properties, showing different characteristics with different fungal species. The fluorescence fingerprint provides a theoretical basis for fungal identification. The spectral differences observed in different fungal structures and in different species is closely related to the material composition and metabolic state of the fungus.

In this study, we proposed the use of SFEFS for diagnosing dermatophytosis. An HFM was fabricated to capture hyperspectral fluorescence images of dermatophytosis specimens. The samples included the common dermatophytes, *Aspergillus, Trichophyton rubrum, Microsporum gypseum*, and *Microsporum canis*. The bright-field and narrow spectral bands of the micro-structure of the dermatophytes were acquired. We compared the effects of bright-field imaging and fluorescence imaging. We observed that fluorescence imaging showed better contrast, which could improve the sensitivity of dermatophyte detection. Meanwhile, the single fungus spectrum of the dermatophytosis specimens was extracted from the hyperspectral fluorescence images. Using a combination of the micro-structure and the single fungus spectrum allows dermatologists to perform morphological and histological analyses from a new angle. Based on experimental data, this method showed high sensitivity and specificity for diagnosing dermatophytosis. Since the biological tissue samples did not needed to be dyed, the operational steps in the process were simplified, therefore reducing overall time and cost of the methodology. Compared to the traditional Wood's lamp, HFM can offer microscopic images and quantitative spectral information for a single fungus and can supply reliable diagnostic information for the dermatologist.

In conclusion, single fungus endogenous fluorescence spectrometry based on hyperspectral fluorescence microscopy could supply reliable diagnostic information for the dermatologist, and this method is a promising low-cost and propagable method for diagnosing dermatophytosis.

Funding

National Natural Science Foundation of China (NSFC) (No. 61475064, 81701743).

Disclosures

The authors declare that there are no conflicts of interest related to this article.